spectrum contains no well-defined maxima (Table III).[18]

Lack of Activity in Initiators for Phenolic Oxidative Coupling. Like other tetranuclear (μ-oxo) complexes, complexes IV–XVII of this study are not initiators for the oxidative coupling of phenols by dioxygen under standard conditions.[3,4]

Acknowledgment. Financial support from the Department of Health and Human Services (Grant RR07143) is gratefully acknowledged. We also thank Professor W. H. Orme-Johnson and co-workers for assistance in obtaining low-temperature spectra at MIT and Professor A. W. Addison for valuable discussions.

Registry No. I (M = Co), 54166-06-2; I (M = Ni), 34214-73-8; I (M = Zn), 72871-59-1; III, 80301-55-9; IV, 102109-29-5; IV·2C_2H_5OH, 102109-30-8; V, 102132-55-8; XVII, 102132-56-9.

Supplementary Material Available: Table III, spectral data (2 pages). Ordering information is given on any current masthead page.

Contribution from the Department of Chemistry,
National Tsing Hua University, Hsinchu, Taiwan 300, Republic of China

Dissociation and Isomerization Kinetics of (*C-meso*-5,5,7,12,12,14-Hexamethyl-1,4,8,11-tetraazacyclotetradecane)copper(II) (Red) Cation in Strongly Acidic, Aqueous Media

Jy-Wann Chen, Der-Shin Wu, and Chung-Sun Chung*

Received June 11, 1985

In order to investigate the effect of structure variation upon complex dissociation rate constants, the kinetics of the dissociation and isomerization of (*C-meso*-5,5,7,12,12,14-hexamethyl-1,4,8,11-tetraazacyclotetradecane)copper(II) (red) cation has been examined spectrophotometrically at 25 °C in 0.1–5.0 M HNO_3. The possible pathways for the cleavages of the copper–nitrogen bonds, the factors influencing the dissociation rates, and the factors affecting the relative importance of each of these possible pathways are considered.

Introduction

Previously, we have reported the dissociation kinetics of the blue copper(II) complexes of tetraamine macrocyclic ligands, *C-meso*- and *C-rac*-5,5,7,12,12,14-hexamethyl-1,4,8,11-tetraazacyclotetradecane, tet a (I) and tet b (II), in strongly acidic, aqueous media.[1,2]

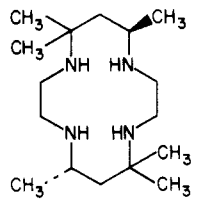

I

tet a or *meso*-1,7-CTH

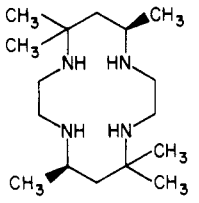

II

tet b or *rac*-1,7-CTH

In the current investigation, we have attempted to gain more detailed understanding of the effect of structure variation on the kinetics of acid-catalyzed dissociation of macrocyclic ligand complexes. To accomplish this, we have extended our studies to the reaction of the red copper(II) complex of tet a in strongly acidic, aqueous media. The crystal structure determinations of $[Cu(tet\ a)\ (blue)]^{2+}$, $[Cu(tet\ a)\ (red)]^{2+}$, and $[Cu(tet\ b)\ (blue)]^{2+}$ have been reported,[3-6] thus providing the opportunity to elaborate the ways in which the different structures of the coordinated macrocyclic tetraaza ligands convey properties on the acid-assisted dissociation kinetics of their metal complexes.

Experimental Section

Reagents. The macrocyclic ligand tet a was prepared by using the procedure described by Hay, Lawrence, and Curtis.[7] The complex $[Cu(tet\ a)\ (red)](ClO_4)_2$ used is the same as that reported earlier.[8-10] All other chemicals used in this work were of GR grade (Merck or Fluka).

Protonation Constant Determinations. For pH measurements a Radiometer PHM 64 equipped with a GK 2401B combined electrode was used. The pH was standardized with NBS buffers. The hydrogen ion and hydroxide ion concentrations in 0.1 M $NaNO_3$ were calculated from $-\log [H^+] = pH - 0.11$ and $pK_w = 13.78$.[11] Above pH 12, the readings were corrected by using standard NaOH solutions to give the hydroxide ion concentration.

Appropriate aliquots of standard solutions of acidic ligand were titrated with a standard sodium hydroxide solution. In all titrations the ionic strength was maintained relatively constant by using 0.1 M $NaNO_3$ as supporting electrolyte. The solutions were protected from air by a stream of humidified prepurified nitrogen and were maintained at 25.0 ± 0.1 °C during measurements.

Kinetic Measurements. Kinetic runs were initiated by mixing a freshly prepared $[Cu(tet\ a)\ (red)](ClO_4)_2$ solution with a solution that contained the desired quantities of HNO_3 and $NaNO_3$. All samples were then well mixed and transferred to a thermostated quartz cell sealed with Teflon. These reactions were followed spectrophotometrically by repetitive scanning through the range 360–700 nm, with particular focus on 504 nm (a maximum for $[Cu(tet\ a)\ (red)]^{2+}$). A Perkin-Elmer Lambda-5 UV–vis spectrophotometer was used for all the solutions studied. The rate constants were obtained by using the CDC Cyber-172 computer.[1]

Results

The electronic spectrum of $[Cu(tet\ a)\ (red)]^{2+}$ has been reported.[1] The kinetics of the dissociation reactions of this complex were studied spectrophotometrically in 0.1–5.0 M HNO_3 (eq 1).

$$[Cu(tet\ a)\ (red)]^{2+} + 4H^+ \rightarrow Cu^{2+} + (H_4tet\ a)^{4+} \quad (1)$$

This process was not found to occur by a single stage but to take place in consecutive–concurrent steps. The isomerization between the red and the blue species also occurs concurrently with its

(1) Liang, B.-F.; Chung, C.-S. *Inorg. Chem.* **1981**, *20*, 2152–2155.
(2) Liang, B.-F.; Chung, C.-S. *Inorg. Chem.* **1983**, *22*, 1017–1021.
(3) Bauer, R. A.; Robinson, W. R.; Margerum, D. W. *J. Chem. Soc., Chem. Commun.* **1973**, 289–290.
(4) Clay, R. M.; Murray-Rust, P.; Murray-Rust, J. *J. Chem. Soc., Dalton Trans.* **1979**, 1135–1139.
(5) Sheu, H.-R.; Lee, T.-J.; Lu, T.-H.; Liang, B.-F.; Chung, C.-S. *Proc. Natl. Sci. Counc., Repub. China* **1983**, *7(2)*, 113–118.
(6) Lee, T.-J.; Lee, H. Y. J.; Lee, C.-S.; Chung, C.-S. *Acta Crystallogr., Sect. C: Cryst. Struct. Commun.* **1984**, *C40*, 641–644.
(7) Hay, R. W.; Lawrance, A. G.; Curtis, N. F. *J. Chem. Soc., Perkin Trans. 1* **1975**, 591–593.
(8) Liang, B.-F.; Chung, C.-S. *J. Chin. Chem. Soc. (Taipei)* **1979**, *26*, 93–99.
(9) Liang, B.-F.; Chung, C.-S. *Inorg. Chem.* **1980**, *19*, 572–574.
(10) Liang, B.-F.; Chung, C.-S. *Inorg. Chem.* **1980**, *19*, 1867–1871.
(11) Liang, B.-F.; Margerum, D. W.; Chung, C.-S. *Inorg. Chem.* **1979**, *18*, 2001–2007.

0020-1669/86/1325-1940$01.50/0

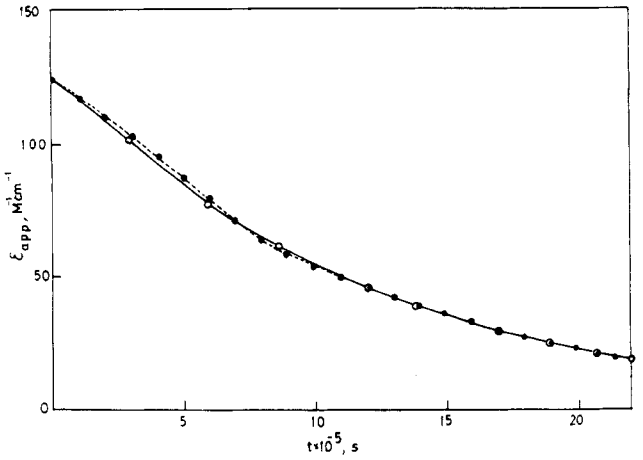

Figure 1. Apparent molar absorptivities vs. time for the reaction of [Cu(tet a) (red)]$^{2+}$ in 4 M HNO_3 (μ = 5.0 M) at 504 nm and 25.0 °C. The solid line is the experimental curve, and the dashed line is the best-fit curve calculated with the constants listed in Table I, $\epsilon_{app} = A_{obsd}/bC_T$.

Table I. Consecutive–Concurrent First-Order Rate Constants for the Dissociation and Isomerization of [Cu(tet a) (red)]$^{2+}$ Cation at 25.0 °C and μ = 5.0 M (HNO_3 + $NaNO_3$)

[HNO_3], M	$10^8k_1^r$, s^{-1}	$10^3k_{-1}^r$, s^{-1}	$10^4k_1^b$, s^{-1}	$10^3k_{-1}^b$, s^{-1}	10^4k_2, s^{-1}
0.1	0.17	2.50	0.34	1.35	4.32
0.2	0.51	2.51	0.73	1.38	4.42
0.5	0.93	2.53	1.50	1.40	4.46
0.8	1.74	2.52	2.25	1.41	4.46
1.0	2.17	2.60	2.70	1.43	4.59
1.5	3.42	2.56	4.12	1.40	4.64
2.0	4.56	2.50	5.74	1.36	4.66
2.5	5.61	2.50	6.50	1.38	4.68
3.0	6.42	2.55	7.87	1.34	4.73
3.5	7.88	2.49	9.42	1.28	4.81
4.0	9.63	2.52	11.30	1.32	4.88
4.5	10.30	2.48	12.60	1.25	4.93
5.0	11.70	2.45	14.20	1.23	5.00

Table II. Pseudo-First-Order Rate Constants as a Function of Acid Concentration at 25.0 °C and μ = 5.0 M (HNO_3 + $NaNO_3$)

k_1^r	2.27 (±0.10) × 10^{-8}[H^+] M^{-1} s^{-1}
k_{-1}^r	2.52 (±0.10) × 10^{-3} s^{-1}
k_1^b	2.70 (±0.20) × 10^{-4}[H^+] M^{-1} s^{-1}
k_{-1}^b	1.34 (±0.10) × 10^{-3} s^{-1}
k_2	1.03 (±0.10) × 10^{-5}[H^+] M^{-1} s^{-1} + 4.46 (±0.20) × 10^{-4} s^{-1}

dissociation.[1] The apparent molar absorptivity vs. time profile for a typical reaction in 4 M HNO_3 (μ = 5.0 M $NaNO_3$ + HNO_3) at 504 nm and 25.0 °C is shown in Figure 1. The kinetic scheme that can accommodate our observations is given in eq 2.

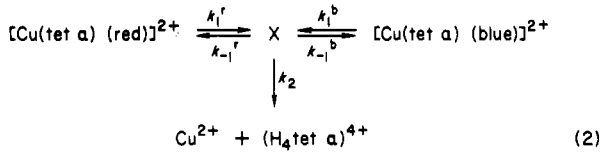

(2)

Here X is an intermediate, and k_1^r, k_{-1}^r, k_1^b, k_{-1}^b, and k_2 are first-order or pseudo-first-order rate constants.

The approximate values of the rate constants were estimated from kinetic measurements. The approximate molar absorptivity of X, ϵ_X, was guessed from scanning spectra. Rodiguin–Rodiguina integration[12] would give the values of the concentrations of [Cu(tet a) (blue)]$^{2+}$, X, [Cu(tet a) (red)]$^{2+}$, Cu^{2+}, and $(H_4tet\ a)^{4+}$ as a function of time. A comparison of the calculated values of absorbances with the observed values, followed by a variation of the rate constants and ϵ_X so as to obtain a minimum deviation between observed and calculated values, would lead to the correct rate constants. The values of ϵ_X at 504 nm, evaluated with the use of computer programs, is 110 ± 15 cm^{-1} M^{-1} in the range 0.1–5.0 M HNO_3 (μ = 5.0 M). Resulting values of these rate constants as a function of acid concentration are given in Table I. One of these experimental curves and the best-fit curve in 4.0 M HNO_3, calculated with rate constants listed in Table I, are shown in Figure 1. The other curves in the range 0.1–5.0 M HNO_3 are very similar to this particular curve.

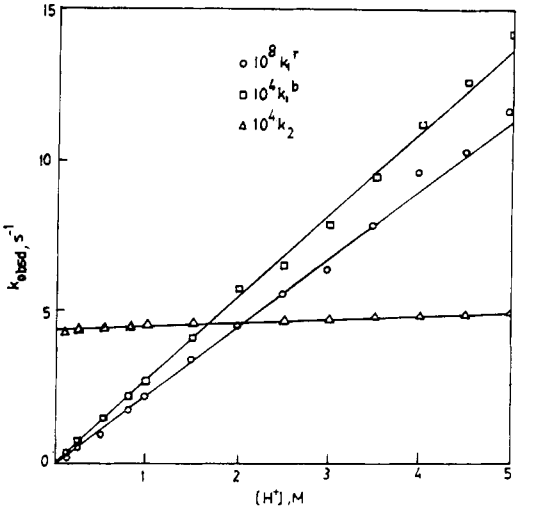

Figure 2. Plots of k_1^b, k_1^r, and k_2 vs. [H^+].

Table III. Protonation Constants of tet a at 25.0 °C and μ = 0.1 M ($NaNO_3$)

log K_1^H	log K_2^H	log K_3^H	log K_4^H
11.9	10.6	2.4	2.1
12.6[a]	10.4[a]	0.8[a]	0[a]

[a] Reference 13.

Table IV. Relative Stability Constants of [Cu(tet a) (red)]$^{2+}$, [Cu(tet a) (blue)]$^{2+}$, and [Cu(Htet a)]$^{3+}$ at 25.0 °C and μ = 5.0 M (HNO_3 + $NaNO_3$)

reacn	equil const	value
[Cu(Htet a)]$^{3+}$ ⇄ [Cu(tet a) (red)]$^{2+}$ + H^+	$K_{R/X}$	1.1 × 10^5 M
[Cu(Htet a)]$^{3+}$ ⇄ [Cu(tet a) (blue)]$^{2+}$ + H^+	$K_{B/X}$	5.0 M
[Cu(tet a) (blue)]$^{2+}$ ⇄ [Cu(tet a) (red)]$^{2+}$	$K_{R/B}$	2.2 × 10^4
		$10^{8\,a}$
		3.2 × $10^{2\,b}$

[a] Reference 13, 0.1 M ionic strength. [b] Reference 4, 0.1 M ionic strength.

The results given in Table I indicate that k_1^r, k_1^b, and k_2 are [H^+] dependent. Plots of these rate constants against [H^+] give straight lines as shown in Figure 2. The values for these measured stepwise rate constants are tabulated in Table II. These results are in excellent agreement with those obtained by using [Cu(tet a) (blue)]$^{2+}$ as starting material under the same conditions.[1]

The values of the protonation constants of this ligand obtained in this work and those reported by Cabbiness and Margerum[13] are summarized in Table III.

The relative stabilities of [Cu(tet a) (red)]$^{2+}$, [Cu(tet a) (blue)]$^{2+}$, and the intermediate, [Cu(Htet a)]$^{3+}$, obtained from the kinetic results are listed in Table IV, together with the reported values determined by other methods.[4,13]

Discussion

The X-ray crystal structure determinations of both the red and the blue complexes of [Cu(tet a)]$^{2+}$ have been reported.[4] The

(12) Rodiguin, N. M.; Rodiguina, E. N. *Consecutive Chemical Reactions*; Van Nostrand: Princeton, NJ, 1964.

(13) Cabbiness, D. K.; Margerum, D. W. *J. Am. Chem. Soc.* **1969**, *91*, 6540–6541.

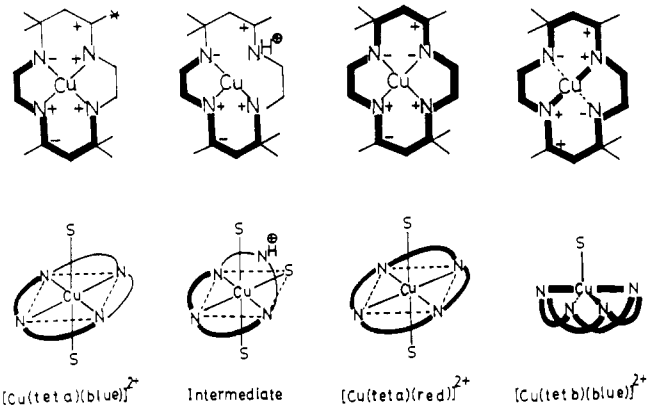

Figure 3. Configurations of the asymmetric centers and the conformations of the chelate rings of $[Cu(tet\ a)\ (blue)]^{2+}$, intermediate, $[Cu(tet\ a)\ (red)]^{2+}$, and $[Cu(tet\ b)\ (blue)]^{2+}$. A plus sign at an asymmetric center indicates that the hydrogen atom of the center is above the plane of the macrocycle, and a minus sign indicates that it is below. Gauche conformations of the five-membered chelate rings and chair conformations of the six-membered chelate rings are indicated by heavier lines. The axial C(7) methyl group is indicated with an asterisk.

configurations of the asymmetric centers and the conformations of the chelate rings of these isomers are shown in Figure 3. As shown in this figure, the blue species of $[Cu(tet\ a)]^{2+}$ differs from the stable red species in the configuration of a single chiral nitrogen center. The possible structure of X, the intermediate in which one metal–amine bond is broken, is shown in Figure 3.

The red form of $[Cu(tet\ a)]^{2+}$ is more stable than the blue one by a factor of 2.2×10^4 (Table IV). There are three important factors influencing the relative stability of these copper(II) complexes, namely the conformational energies of the chelate rings, the ligand field stabilization energies (LFSE) of these complexes, and the tendency for axial coordination with solvent. As shown in Figure 3, the red form of $[Cu(tet\ a)]^{2+}$ contains four stable chelate rings, two chair forms of the six-membered chelate rings, and two gauche forms of the five-membered chelate rings. On the other hand, the blue form contains two unstable chelate rings.[4] Furthermore, the electronic absorption spectra of these complexes indicate the LFSE of the red form is much larger than that of the blue form.[1] Although the blue form has a larger tendency for axial coordination with solvent than the red form,[9] both the LFSE and the conformational energies of the chelate rings promote the formation of $[Cu(tet\ a)\ (red)]^{2+}$. As a result, $K_{R/B}$ is very large.

The intermediate, $[Cu(Htet\ a)]^{3+}$, is relatively unstable as compared to $[Cu(tet\ a)\ (red)]^{2+}$. The main cause of the instability of the intermediate is due to the large electrostatic effect. In view of the constraints of a cyclic structure, it is apparent that the protonated amine group and the metal ion in $(Cu(Htet\ a)]^{3+}$ are very close, resulting in a large $K_{R/X}$ (Table IV).

A comparison between the relative rate (k_1^r/k_1^b) and the relative stability ($K_{R/B}$) constants indicates that the first Cu–N bond is fully broken in the transition states for reactions 3 and 4. Thus,

$$[Cu(tet\ a)\ (red)]^{2+} + H^+ \rightarrow [Cu(Htet\ a)]^{3+} \quad (3)$$

$$[Cu(tet\ a)\ (blue)]^{2+} + H^+ \rightarrow [Cu(Htet\ a)]^{3+} \quad (4)$$

there are two types of mechanistic pathways for the cleavage of the first copper–nitrogen bond in strongly acidic, aqueous media: one is the direct protonation pathway and the other is the solvation or solvent-separation pathway.[14,15] In the direct protonation pathway, Cu–N bond breaking and direct protonation of the nitrogen donor occur first, with rapid metal ion solvation occurring in a second step; in the solvation or solvent-separation pathway, Cu–N bond breaking and metal ion solvation occur first, with rapid

(14) Margerum, D. W.; Cayley, G. R.; Weatherburn, D. C.; Pagenkopf, G. K. *ACS Monogr.* **1978**, *No. 174*, 1–220.
(15) Read, R. A.; Margerum, D. W. *Inorg. Chem.* **1981**, *20*, 3143–3149.

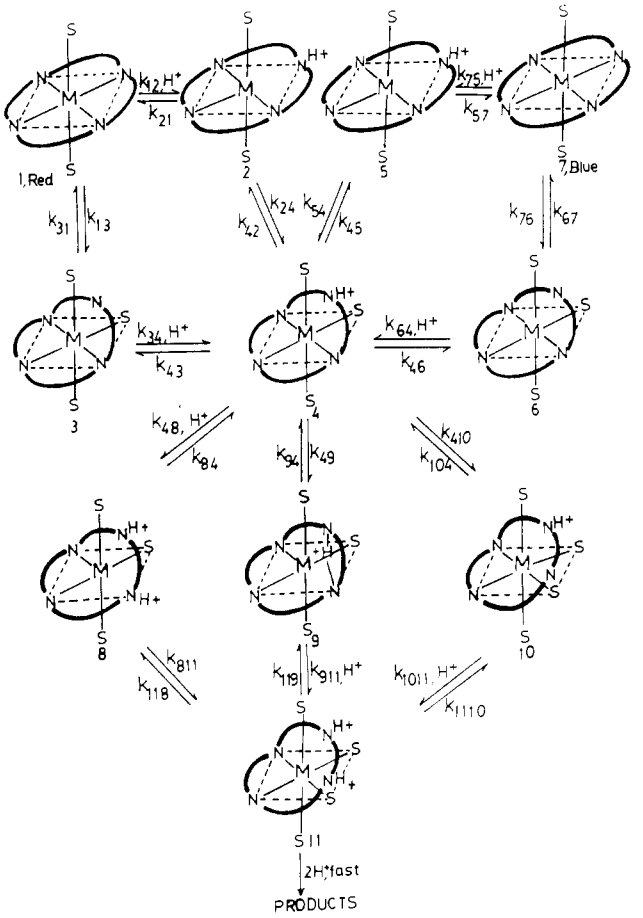

Figure 4. Proposed stepwise mechanism for the dissociation and the isomerization of $[Cu(tet\ a)\ (red)]^{2+}$ in strongly acidic media.

Table V. Summary of Measured Rate Constants Defined in Terms of the Rate Constants for Individual Steps in Figure 4 in the Dissociation of $[Cu(tet\ a)]^{2+}$ at 25.0 °C and μ = 5.0 M (HNO_3 + $NaNO_3$)

k_{1H}^r, $M^{-1}\ s^{-1}$	k_{12}	2.27×10^{-8}
k_{-1H}^r, s^{-1}	$(k_{21}k_{42})/k_{24}$	2.52×10^{-3}
k_{1H}^b, $M^{-1}\ s^{-1}$	k_{75}	2.70×10^{-4}
k_{-1H}^b, s^{-1}	$(k_{57}k_{45})/k_{54}$	1.34×10^{-3}
k_{2H}, $M^{-1}\ s^{-1}$	k_{48}	1.03×10^{-5}
k_{2d}, s^{-1}	$(k_{49} + k_{410})$	4.46×10^{-4}

Table VI. Rate Constant Ratios Representing the Relative Importance of the Pathways for the Dissociation Reactions of Copper(II) Macrocyclic Tetraamine Complexes

$[ML]^{2+}$	k_{1H}/k_{1d}, M^{-1}	k_{2H}/k_{2d}, M^{-1}
$[Cu(tet\ a)\ (red)]^{2+}$	very large	0.023
$[Cu(tet\ a)\ (blue)]^{2+}$	very large	0.023
$[Cu(tet\ b)\ (blue)]^{2+}$ [a]	2.7	0.15

[a] Reference 2.

protonation of the nitrogen donor occurring in a second step as shown in Figure 4. In this figure, species **1**, **4**, and **7** are $[Cu(tet\ a)\ (red)]^{2+}$, intermediate $[Cu(Htet\ a)]^{3+}$, and $[Cu(tet\ a)\ (blue)]^{2+}$, respectively. In strongly acidic media, $k_{24} >> k_{21}$, $k_{34}[H^+] >> k_{31}$, $k_{54} >> k_{57}$, and $k_{64}[H^+] >> k_{67}$, so that

$$k_1^r = k_{1H}^r[H^+] + k_{1d}^r = k_{12}[H^+] + k_{13} \quad (5)$$

$$k_{-1}^r = k_{-1H}^r + \frac{k_{-1d}^r}{[H^+]} = \frac{k_{21}k_{42}}{k_{24}} + \frac{k_{43}k_{31}}{k_{34}[H^+]} \quad (6)$$

$$k_1^b = k_{1H}^b[H^+] + k_{1d}^b = k_{75}[H^+] + k_{76} \quad (7)$$

$$k_{-1}^b = k_{-1H}^b + \frac{k_{-1d}^b}{[H^+]} = \frac{k_{57}k_{45}}{k_{54}} + \frac{k_{46}k_{67}}{k_{64}[H^+]} \quad (8)$$

The measured and the corresponding mechanistic rate constants are listed in Table V.

The relative rate of the cleavage of the M–N bond by the protonation and the solvation pathways, represented by the ratio k_{1H}^{r}/k_{1d}^{r}, is of interest and is significant.[15] The values of these ratios and those for the dissociation of [Cu(tet b) (blue)]$^{2+}$ reported previously[2] are summarized in Table VI. For the cleavage of the first M–N bond, there are four important factors affecting the ratio k_{1H}/k_{1d}: (a) the restriction of the polydentate ligand to prevent the donor from moving out of the first coordination sphere; (b) the coordination number and the configuration of the complex; (c) steric effects; (d) a hydrophobic bonding effect. As pointed out by Read and Margerum,[15] if the donor is unrestricted and able to move easily out of the first coordination sphere, the presence of acid has little effect. However, if the movement of the donor away from the metal ion is hindered in some way, acid can enhance the rate of dissociation. For the cleavage of the first metal–nitrogen bond, the restrictions imposed by the ligand cyclization serve to hold the donor in the first coordination sphere, making the macrocyclic complex more susceptible to acid attack than the corresponding open-chain complex, which has a much smaller restriction of the chelate ring to prevent the donor from moving smoothly out of the first coordination sphere. As a result, the ratio k_{1H}/k_{1d} for the macrocyclic complex is much larger than that for the corresponding open-chain complex.

As the coordination number of the complex decreases, the complex is open to solvent attack, the presence of acid has little effect, and the ratio k_{1H}/k_{1d} is relatively small. On the other hand, as the coordination number of the complex increases, the solvent attack at the metal ion is hindered, acid can enhance the rate of dissociation, and the ratio k_{1H}/k_{1d} is large. The coordination about Cu(II) in [Cu(tet a) (blue)]$^{2+}$ or [Cu(tet a) (red)]$^{2+}$ is a tetragonally distorted octahedron with the macrocyclic ligand equatorial and two water molecules axial.[4] Solvent attack at the metal ion of these complexes is highly hindered. In marked contrast to the behavior of [Cu(tet a) (blue)]$^{2+}$ and [Cu(tet a) (red)]$^{2+}$, the folded five-coordinated trigonal-bipyramidal [Cu(tet b) (blue)]$^{2+}$ is susceptible to solvent attack.[2,3] Therefore, the value of the k_{1H}/k_{1d} ratio for [Cu(tet b) (blue)]$^{2+}$ is much smaller than those of [Cu(tet a) (red)]$^{2+}$ and [Cu(tet a) (blue)]$^{2+}$ (Table VI).

Solvent attack at the metal ion of [Cu(tet a) (red)]$^{2+}$ or [Cu(tet a) (blue)]$^{2+}$ is hindered by both the steric effects and the hydrophobic bonding effect due to the macrocyclic ligand. All these four factors lead to an extremely small k_{1d} value and a very large k_{1H}/k_{1d} ratio for the dissociation of [Cu(tet a)(red)]$^{2+}$ or [Cu(tet a) (blue)]$^{2+}$. The fact that k_{1d}^{r} and k_{1d}^{b} do not significantly contribute to the observed rates substantiates this expectation. These considerations and the large k_{1H}^{b}/k_{1H}^{r} ratio indicate the protonation pathway for the cleavage of the first Cu–N bond in [Cu(tet a) (red)]$^{2+}$ or [Cu(tet a) (blue)]$^{2+}$ exhibits dissociative character.

For the cleavage of the second Cu–N bond, there are three possible pathways as shown in Figure 4. In addition to the protonation and solvation pathways discussed above, a third type of pathway, an intramolecular H-bonding pathway, contributes to the rate. In this pathway, Cu–N bond breaking and intramolecular H-bonding formation occur first, with rapid protonation of nitrogen donor and metal ion solvation occurring in a second step.

In strongly acidic media, $k_{811} >> k_{84}$, $k_{911}[H^+] >> k_{94}$, and $k_{1011}[H^+] >> k_{104}$ (Figure 4), so that

$$k_2 = k_{2H}[H^+] + k_{2d} = k_{48}[H^+] + k_{49} + k_{410} \qquad (9)$$

The measured and the corresponding mechanistic rate constants are listed in Table V.

In general, the ratio k_{2H}/k_{2d} for the cleavage of the second M–N bond is smaller than the ratio k_{1H}/k_{1d} for the cleavage of the first M–N bond. The usual causes for the smaller k_{2H}/k_{2d} ratio compared with k_{1H}/k_{1d} for the dissociation of a metal polyamine complex are two: (a) electrostatic effects; (b) the formation of intramolecular hydrogen bonding after the cleavage of the second M–N bond. These two causes play much more important roles in the dissociation reactions of macrocyclic polyamine complexes than in the dissociation reactions of open-chain polyamine complexes. It is apparent that the constraints of the cyclic structure decrease the distances among the two protonated sites on the ligand and metal ion in species **8** in Figure 4, resulting in extremely large electrostatic replusions. Therefore, the protonation pathway for the cleavage of the second M–N bond is highly hindered by the electrostatic effects. The extremely small third and fourth protonation constants listed in Table III also reflect these extremely large electrostatic repulsions.

The tendency to form intramolecular hydrogen bonds within a macrocyclic polyamine is much larger than that between the amino groups of an open-chain polyamine.[16,17] There are several degrees of freedom of internal rotational entropy lost for each intramolecular hydrogen bond formed between the amino groups of an open-chain polyamine. On the other hand, there is no such internal rotational entropy lost for the formation of intramolecular hydrogen bond within a macrocyclic polyamine. The large first and second protonation constants listed in Table III also indicate that the tendency to form intramolecular hydrogen bonds within (Htet a)$^+$ and (H_2tet a)$^{2+}$ is large.

On the basis of these analyses, the direct protonation pathway for the cleavage of the second Cu–N bond of these complexes is highly hindered by the electrostatic effects; the solvation pathway is hindered by the restriction of ligand cyclization, steric effects, and a hydrophobic bonding effect. On the contrary, the intramolecular H-bonding pathway is accelerated by the large tendency to form an intramolecular hydrogen bond within the macrocyclic ligand.[17] We may expect that the cleavage of the second Cu–N bond of macrocyclic complexes is mainly via this pathway. The fact that the ratio k_{2H}/k_{2d} is very small substantiates this expectation.

Acknowledgment. This work was supported by a grant from the Chemistry Research Center, National Science Council of the Republic of China, for which the authors express their thanks.

Registry No. [Cu(tet a) (red)]$^{2+}$, 24830-76-0.

(16) Liu, Landie; Wu, J.-C.; Chung, C.-S. *J. Chin. Chem. Soc. (Taipei)* **1984**, *31*, 15–21.
(17) Luo, C.-L.; Chin, C.-H.; Chung, C.-S. *J. Chin. Chem. Soc. (Taipei)* **1979**, *26*, 61–69.